12. K. Farmer, F. Catala, W. E. Wright, *J. Biol. Chem.* **267**, 5631 (1992).
13. R. M. McAllister, J. Melnyk, J. Z. Findelstein, E. C. Adams Jr., M. B. Gardner, *Cancer (Phila.)* **24**, 520 (1969); A. L. Hiti, E. Bogenmann, F. Gonzales, P. A. Jones, *Mol. Cell. Biol.* **9**, 4722 (1989); A. De Chiara, A. T'Ang, T. J. Triche, *J. Natl. Cancer Inst.* **85**, 152 (1993); S. J. Tapscott, M. J. Thayer, H. Weintraub, *Science* **259**, 1450 (1993).
14. M. E. Ewen, B. Faha, E. Harlow, D. M. Livingston, *Science* **255**, 85 (1992); B. Faha, M. E. Ewen, L.-H. Tsai, D. M. Livingston, E. Harlow, *ibid.*, p. 87.
15. H.-J. S. Huang *et al.*, *ibid.* **242**, 1563 (1988).
16. X.-Q. Qin, T. Chittenden, D. M. Livingston, W. G. Kaelin Jr., *Genes Dev.* **6**, 953 (1992).
17. S. L. Amacher, J. N. Buskin, S. D. Hauschka, *Mol. Cell. Biol.* **13**, 2753 (1993).
18. A. Lassar and H. Weintraub, in *Transcriptional Regulation*, S. L. McKnight and K. R. Yamamoto, Eds. (Cold Spring Harbor Laboratory Press, Cold Spring Harbor, NY, 1992), pp. 1037–1061.
19. Although transfection of Rb or p107 was required to activate MCKCAT and induce cell cycle arrest in Saos-2–myogenin cells, these myogenic factor–expressing tumor cells, like RD rhabdomyosarcoma cells, could sporadically express certain endogenous muscle genes.
20. M. C. Cardoso, H. Leonhardt, B. Nadal-Ginard, *Cell* **74**, 979 (1993); R. Maione, G. M. Fimia, P. Holman, B. Schaffhausen, P. Amati, *Cell Growth Diff.* **5**, 231 (1994).
21. $Rb^{-/-}$ and $Rb^{+/-}$ embryonic stem cells (*5*) were grown as subcutaneous teratomas in severe combined immunodeficiency disease mice. Teratomas were explanted after 2 weeks, enzymatically disrupted, and recultured in monolayers in 20% fetal calf serum (FCS) with 1% rat serum in Dulbecco's minimum essential medium (DMEM). Myotube formation was induced by depletion of growth factors in 5% horse serum in DMEM, and myotubes were subcloned and recultured in 20% FCS for isolation of residual myoblasts. Identical results were obtained in at least three independently cloned $Rb^{-/-}$ teratoma-derived myoblast lines. Immunostaining and BrdU incorporation were done as in (*4, 22*) with the following mAbs and antisera: Rb mAb (PMG3-245; Pharmingen), p107 mAb (SD9), MHC mAb (MF20), myogenin mAb (F5D), 12CA5 hemagglutinin (HA) tag mAb (*9*), bacterial chloramphenicol acetyltransferase (CAT) antiserum (5-Prime 3-Prime), fluorescein-conjugated BrdU mAb (Boehringer), pan-neuronal filament mAb (SMI-311; Sternberger Monoclonals), PCNA mAb Z049 (Zymed), and cyclin D antiserum (UBI); secondary antisera were goat rhodamine-conjugated antibodies to rabbit Ig (Boehringer), goat fluorescein-conjugated antibodies to mouse Ig (Boehringer), rabbit rhodamine-conjugated antibodies to mouse Ig (Dako), or various goat antibodies to specific isotypes of mouse Ig conjugated to fluorochromes (Boehringer). Nuclei were counterstained with Hoechst 33258 (Sigma).
22. V. Sorrentino, R. Pepperkok, R. L. Davis, W. Ansorge, L. Phillipson, *Nature* **345**, 813 (1990); M. Crescenzi, T. P. Fleming, A. B. Lassar, H. Weintraub, S. A. Aaronson, *Proc. Natl. Acad. Sci. U.S.A.* **87**, 8442 (1990).
23. Protein blots were done as in (*4*) with whole cell extracts in EBC buffer with Rb (PMG3-245) and p107 (SD9) mAbs and the ECL detection system (Amersham). RNA blots were done with polyadenylated RNA prepared as in (*24*) with Nytran (Schleicher & Schuell); equivalent loading was verified by methylene blue staining of the filters as in (*24*). The following complementary DNA (cDNA) fragments were used as probes: full-length human Rb from pCMV-Rb (*16*), 1.2-kb (Bam HI–Dra III) 5′-subfragment of human p107 from pCMV-p107 (*9*), and full-length murine MyoD and myogenin, rat skeletal MHC, and human p53, as described in (*25*).
24. J. Sambrook, E. F. Fritsch, T. Maniatis, *Molecular Cloning: A Laboratory Manual* (Cold Spring Harbor Laboratory, Cold Spring Harbor, NY, 1989).
25. R. L. Davis, H. Weintraub, A. B. Lassar, *Cell* **51**, 987 (1987); W. E. Wright, D. A. Sassoon, V. K. Lin, *ibid.* **56**, 607 (1989); L. G. Garfinkel, M. Periasamy, B. Nadal-Ginard, *J. Biol. Chem.* **257**, 11078 (1982); S. J. Baker, S. Markowitz, E. R. Fearon, J. K. V. Willson, B. Vogelstein, *Science* **249**, 912 (1990).
26. The GST binding experiments and coimmunoprecipitation protein blots were done as in (*4*). GST-Id contained full-length mouse Id and GST–E-protein contained the bHLH domain of human E2-2.
27. We thank H. te Riele and A. Berns for providing the $Rb^{-/-}$ and $Rb^{+/-}$ embryonic stem cells, M. Ewen for GST-p107, W. Kaelin for pCMV-Rb, J. Buskin for pMCKCAT, B. Vogelstein for pCMV-Neo-Bam, N. Dyson for SD9 mAb, W. Wright for F5D mAb, D. Bader for MF20 mAb, and E. Ferris for technical assistance. Supported by grants from NIH, the Muscular Dystrophy Association of America, the Howard Hughes Medical Institute, and the MERCK/American Federation for Clinical Research (J.W.S.).

22 October 1993; accepted 15 April 1994

Inhibition of Hepatic Chylomicron Remnant Uptake by Gene Transfer of a Receptor Antagonist

Thomas E. Willnow, Zeqi Sheng, Shun Ishibashi, Joachim Herz*

The low density lipoprotein receptor-related protein (LRP) has been proposed to mediate in concert with the LDL receptor (LDLR) the uptake of dietary lipoproteins into the hepatocytes. This hypothesis was tested by transient inactivation of LRP in vivo. Receptor-associated protein (RAP), a dominant negative regulator of LRP function, was transferred by an adenoviral vector to the livers of mice lacking LDLR ($LDLR^{-/-}$). The inactivation of LRP by RAP was associated with a marked accumulation of chylomicron remnants in $LDLR^{-/-}$ mice and to a lesser degree in normal mice, suggesting that both LDLR and LRP are involved in remnant clearance.

Apolipoprotein E (apoE) and apoB48 (a truncated form of apoB100) are constituents of chylomicron remnants, the carriers of dietary cholesterol. Whereas apoB48 is primarily a structural component of these lipoproteins, apoE is required for their receptor-mediated endocytosis in the liver (*1, 2*). Two hepatic receptors are known to bind apoE-containing lipoproteins: LDLR and LRP. Experiments performed in vitro and in intact animals demonstrate that LDLR binds to and takes up chylomicron remnants (*3, 4*). However, humans, rabbits, and mice lacking functional LDLR do not accumulate chylomicron remnants in their circulation (*5, 6*). It was therefore suggested that LRP also is involved in chylomicron remnant clearance and that it substitutes for LDLR when the latter is deficient (*7, 8*). This proposed function of LRP has been impossible to prove in a physiological experiment because embryos lacking LRP fail to develop in utero (*9*). Embryonic lethality probably occurs because LRP is a multifunctional receptor that not only participates in lipid metabolism but also is involved in the uptake of extracellular proteases, the protease inhibitor α_2-macroglobulin, and other macromolecules (*10, 11*). This precludes the analysis of remnant metabolism in animals that are genetically deficient in LRP.

One way to circumvent this problem is to administer a specific inhibitor of LRP. A candidate inhibitor is a receptor-associated protein (RAP) of approximately 39 kD that copurifies with LRP (*10*). When added to cultured cells or to purified receptor, RAP binds to LRP at multiple sites and blocks ligand-receptor interaction (*12–15*). In the current study we used an adenovirus vector to carry a RAP complementary DNA (cDNA) into the liver of adult mice in order to test the hypothesis that RAP overproduction would inactivate LRP and cause chylomicron remnants to accumulate in the circulation. Recombinant adenoviruses have proven to be efficient gene transfer vectors that preferentially target hepatocytes when injected intravenously into animals (*6, 16, 17*). As recipient animals we have used wild-type (+/+) mice and mice that lack LDL receptors ($LDLR^{-/-}$) as a result of targeted gene disruption. The latter mice have elevated levels of LDL but no gross accumulation of chylomicron remnants when fed a normal Chow diet (*6*).

Recombinant adenoviruses containing either the RAP cDNA (AdCMV-RAP) or the *Escherichia coli* β-galactosidase gene (AdCMV–β-Gal) (*18*) were intravenously injected into wild-type or $LDLR^{-/-}$ mice (*19*). Five days after the injection of the virus, we assessed LRP activity by monitoring the ability of the mice to clear an LRP-specific ligand, ^{125}I-labeled α_2-macroglobulin (^{125}I-α_2M), from their circulation. Other animals were injected with ^{125}I-labeled asialofetuin (^{125}I-ASF), which enters the cell through the asialoglycoprotein re-

Department of Molecular Genetics, University of Texas Southwestern Medical Center, Dallas, TX 75235, USA.
*To whom correspondence should be addressed.

ceptor (*20*). This receptor, also expressed on hepatocytes, is unrelated to LRP.

AdCMV-RAP–injected mice, but not uninjected or AdCMV–β-Gal–injected animals, were unable to clear ^{125}I-α_2M from their circulation (Fig. 1). Animals injected with either virus cleared ^{125}I-ASF almost as efficiently as uninjected controls. The results obtained with both ligands were similar in wild-type and LDLR$^{-/-}$ animals. However, there was a marked difference in the appearance of the plasma between the two strains of mice. Plasma from LDLR$^{-/-}$ mice that had received the RAP virus was distinctly turbid, indicating the presence of light dispersing lipoprotein particles. Plasma from wild-type mice that had received the same virus showed a slight turbidity only on occasion. In no case (n = 46) did we observe such changes in plasma appearance in animals of either genotype that were not injected or were injected with control virus. Consistent with this observation, LDLR$^{-/-}$ mice that had received AdCMV-RAP also had, on average, more than three times the total plasma cholesterol that was observed in animals of the same genotype that had received the control virus or were uninjected (Table 1). Wild-type animals showed only a mild elevation in plasma cholesterol. The increase in plasma triglyceride concentration in AdCMV-RAP–injected mice was quantitatively similar to the increase in plasma cholesterol in the same animals. This suggests that the accumulating lipoproteins consisted of largely lipolysed remnant particles rather than unprocessed chylomicrons, which contain predominantly triglycerides and are relatively poor in cholesterol (*21*).

Total plasma cholesterol of LDLR$^{-/-}$ animals was roughly proportional to the amount of RAP present in plasma (Fig. 2A). Cholesterol levels of wild-type mice that had received AdCMV-RAP were only slightly increased in proportion to the RAP concentration in plasma. The presence of LDLR therefore largely protects wild-type mice from RAP-induced hyperlipidemia. In contrast, the plasma clearance rate of ^{125}I-α_2M (Fig. 2B) was inversely proportional to the plasma RAP concentration in both wild-type and LDLR$^{-/-}$ animals.

To determine which lipoprotein subfraction was responsible for the increased cholesterol levels in AdCMV-RAP–injected LDLR$^{-/-}$ mice, we analyzed the plasma lipoprotein profiles by fast performance liquid chromatography (FPLC) (Fig. 3). The profile of AdCMV–β-Gal–injected mice was similar to that of uninjected animals of the same genotype. The plasma cholesterol of wild-type mice is contained mainly in the high density lipoprotein (HDL) fraction, whereas in LDLR$^{-/-}$ mice 50% or more of the total plasma cholesterol is in the intermediate density (IDL)-LDL size range [Fig. 3 and (*6*)]. LDLR$^{-/-}$ mice injected with AdCMV-RAP and to a much lesser degree wild-type mice injected with the same virus accumulated large cholesterol-rich remnant-sized particles in their plasma with a concomitant reduction in HDL cholesterol.

We next used semiquantitative protein immunoblot analysis to determine whether RAP expression causes a change in the apoprotein profile in the plasma of virus-injected mice (Fig. 4). Both wild-type and LDLR$^{-/-}$ mice that had received AdCMV-RAP accumulated apoB48 and apoE in their plasma as compared with uninjected or AdCMV–β-Gal–injected control animals. In addition, a reduction in the plasma level of apoAI (the major HDL apoprotein) was also apparent in the animals that overexpressed RAP, whereas the concentration of apoB100 in plasma was not affected by either virus, regardless of the genotype of the animals. Thus, the overexpression of RAP primarily affects the apoE-dependent clearance of remnants but not of LDL from the circulation.

Here we have used the term "chylomicron remnant" to refer to lipoproteins that contain apoB48. In humans, all apoB48 is produced in the intestine and secreted in chylomicrons. In mice, however, apoB48 is also made by the liver (*21*) and secreted in very low density lipoproteins (VLDLs). The hepatic and intestinal apoB48-containing particles are physically and functionally indistinguishable.

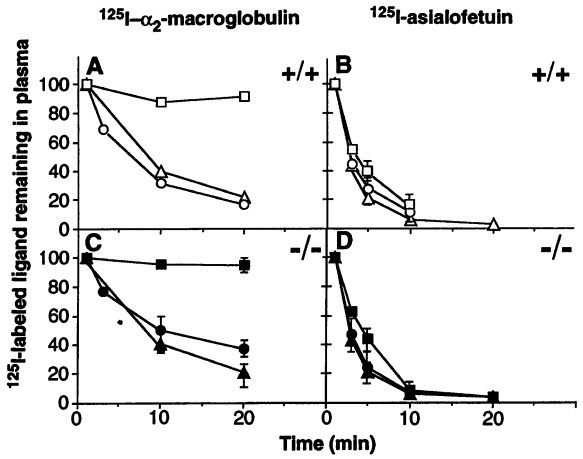

Fig. 1. Plasma clearance of ^{125}I-labeled ligands in virus-injected mice. Either 4 × 10^{11} particles of AdCMV–β-Gal (circles) or 2 × 10^{11} particles of AdCMV-RAP (squares) were injected into the external jugular vein of wild-type (**A** and **B**) or LDLR$^{-/-}$ mice (**C** and **D**). Five days after virus administration the mice received an intravenous injection of either ^{125}I-labeled human α_2M or bovine asialofetuin (5 μg of tracer in 200 μl of tris-buffered saline containing 0.1% bovine serum albumin). At the indicated time points, blood samples (~80 μl) were collected by retro-orbital puncture and the amount of tricholoroacetic acid–precipitable radioactivity in plasma was determined as described (*17*). Mice that had not been injected with virus served as controls (triangles). Values are expressed as the percent of radioactivity present in plasma at 1 min after injection of the label. Variances shown represent the range of absolute values measured (between two and eight mice per group) in 18 different experiments. Where no range bar is shown, the difference between individual data points is smaller than or equal to the size of the respective symbol. In all mice injected with AdCMV-RAP, plasma concentrations of RAP were ≥40 μg/ml (determined as described in Fig. 2).

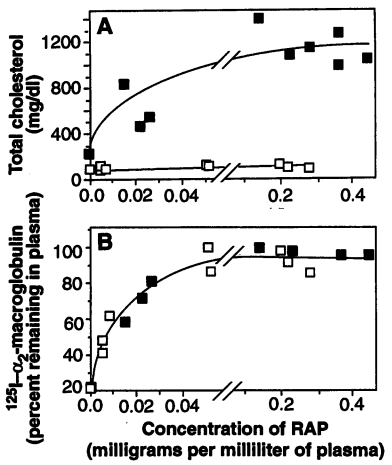

Fig. 2. Hyperlipidemia correlates with reduced α_2M clearance in RAP-overexpressing LDLR$^{-/-}$ but not wild-type mice. Wild-type (open squares) or LDLR$^{-/-}$ mice (closed squares) were injected with 2 × 10^{11} particles of AdCMV-RAP. Five days after virus administration the animals were injected with 5 μg of ^{125}I-α_2M, and plasma radioactivity at 1 and 20 min after injection of the label was determined as described in Fig. 1 except that at 20 min blood (~1 ml) was collected from the vena cava. Concentrations of ^{125}I-α_2M remaining in plasma 20 min after injection of the label are plotted as the percent of the amount present at 1 min. Total plasma cholesterol concentrations were determined enzymatically (*6*). For measurement of RAP concentrations, serial dilutions of plasma samples were separated by SDS–gel electrophoresis on 4 to 15% polyacrylamide gels under reducing conditions and transferred to nitrocellulose. The filters were probed with anti-RAP immunoglobulin G (IgG; 5 μg/ml), and bound IgG was detected with ^{125}I-labeled goat antibody to rabbit IgG. Radioactivity in the individual bands was quantified on a radio analytical imaging detector (AMBIS) and compared to standard amounts of purified RAP on the same blot. Total cholesterol concentrations (**A**) or the amount of ^{125}I-α_2M remaining in the plasma 20 min after injection of the label (**B**) were plotted as a function of the RAP concentration present in the plasma of the individual animals.

Therefore, the remnants that accumulate in the RAP-expressing animals must constitute a mixture of remnants derived from true intestinal chylomicrons and hepatic VLDLs.

An important consideration for the interpretation of the experiments presented here is the well-established cellular toxicity associated with adenovirus-infection of murine tissues (*22*). Histological analysis of the livers of virus-injected animals revealed an inflammatory response marked by lymphocytic infiltrations but no discernible histological difference between livers expressing β-Gal or RAP (*23*). To control for nonspecific virus effects, we first examined the effect of virus infection on the function of another unrelated, well-studied hepatocellular endocytic receptor, the asialoglycoprotein receptor. In contrast to LRP, infection of the mice with AdCMV-RAP did not substantially affect the activity of the asialoglycoprotein receptor. Furthermore, in no case did injection of the mice with AdCMV–β-Gal induce a change of the lipoprotein profile. Another irrelevant virus expressing the firefly luciferase gene (AdCMV-Luc) also had no effect (*23*), in agreement with previous studies (*6*). In all cases, remnant accumulation was solely dependent on RAP expression. The general health and the activity of the animals did not appear to be affected by the virus infection.

A current model for hepatic clearance of chylomicron remnants states that the remnants are first sequestered in the sinusoidal space (*4*), possibly by adsorption to proteoglycans (*24*) and interaction with hepatic lipase (*25*) and LDLR (*3*). After local enrichment of the particle with apoE on the surface of the hepatocytes (*26*), the remnants are internalized by endocytosis, mediated by LDLR and by a second receptor which we believe is LRP. In the current study, RAP overexpression caused an increase in the steady-state concentration of remnant particles in the circulation. If the proteoglycan-sequestration model is correct, our results would suggest that a RAP-mediated block of remnant endocytosis eventually leads to a saturation of this intermediate compartment as the remnants accumulate in the plasma.

The small amount of remnants that accumulated in the normal mice injected with AdCMV-RAP is probably due to a partial inhibition of LDLR at high RAP expression levels in addition to the total block of the alternative remnant clearance pathway. RAP binds weakly to LDLR (*27*).

The physiological role of RAP is not clear at present. Because RAP resides predominantly in the endoplasmic reticulum (*28*), in contrast to LRP which is localized primarily in post-Golgi and recycling compartments (*8*), it has been proposed to function as a fast-acting modulator of LRP activity that can be mobilized from intracellular storage compartments in response to an unknown signal (*13, 14, 29*). In the present experiments, overexpression of RAP from a strong viral promoter resulted in the secretion of RAP into the plasma where it accumulated in concentrations sufficient to directly inhibit LRP (*13*) on the hepatic cell surfaces. Our study does not allow conclusions as to possible effects of RAP overexpression on the intracellular pathway of LRP, which could contribute to the observed functional block of this receptor.

The reasons for the reduction of plasma HDL in RAP-expressing animals (in which chylomicron remnant clearance has been acutely impaired) are not entirely clear. However, cholesterol-fed (*30*) as well as apoE-deficient (*2*) mice (which show a

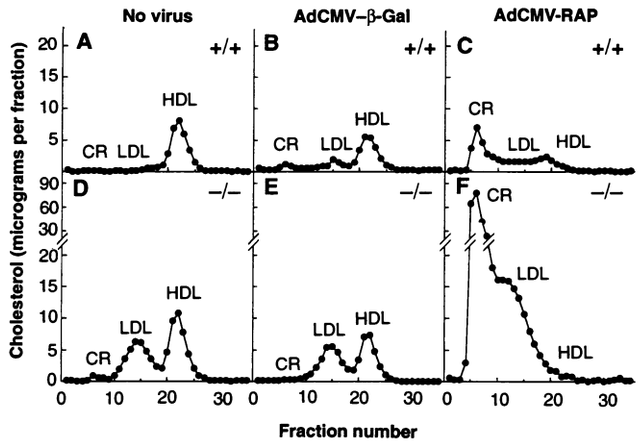

Fig. 3. FPLC profile of mouse lipoproteins. Wild-type (**A** to **C**) or LDLR$^{-/-}$ mice (**D** to **F**) were injected with 4 × 10^{11} particles of AdCMV–β-Gal (B and E) or 2 × 10^{11} particles of AdCMV-RAP (C and F) as described in Fig. 1. Five days after virus administration blood was drawn from the vena cava of the individual animals, and 100 μl plasma was analyzed by FPLC on a Superose 6 column (Sigma) as previously described (*6*). The cholesterol content of each fraction was measured spectrofluorimetrically (*31*). The lipoprotein profiles of noninjected control animals are depicted in (A) and (D). Representative profiles of individual animals of each group (between 3 and 10 animals per group) are shown. Fractions containing VLDL-chylomicron remnants (CR), LDL, and HDL are indicated.

Table 1. Total plasma cholesterol and triglycerides in normal and LDLR$^{-/-}$ uninjected and virus-injected mice. Mice of the indicated genotype were either not injected or injected with AdCMV–β-Gal (~4 × 10^{11} viral particles) or AdCMV-RAP (~2 × 10^{11} viral particles). Total plasma cholesterol and triglyceride concentrations (mean ± SEM) were determined enzymatically 5 days after virus injection (*6*). Total plasma cholesterol and triglyceride concentrations of uninjected and AdCMV–β-Gal–injected mice agree closely with those observed in previous studies (*6, 17*). The number of animals examined in each group is given in parentheses. Significant differences (injected versus noninjected mice of the same genotype) are indicated by the asterisks (*$P \leq 0.05$; **$P \leq 0.005$).

Virus	LDLR$^{+/+}$		LDLR$^{-/-}$	
	Cholesterol (mg/dl)	Triglycerides (mg/dl)	Cholesterol (mg/dl)	Triglycerides (mg/dl)
None	92 ± 9	94 ± 10 (8)	237 ± 22	155 ± 22 (7)
β-Gal	90 ± 4	156 ± 16** (7)	297 ± 13*	234 ± 17* (13)
RAP	150 ± 17*	254 ± 27** (15)	1057 ± 61**	1203 ± 168** (23)

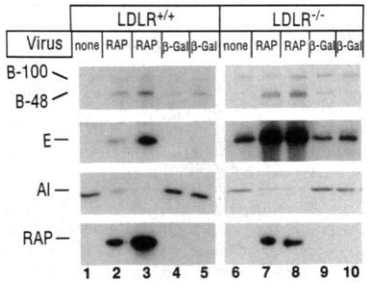

Fig. 4. Immunoblot analysis of mouse apoproteins. Plasma from wild-type (lanes 1 to 5) and LDLR$^{-/-}$ mice (lanes 6 to 10) that were uninjected (lanes 1 and 6) or injected with approximately 4 × 10^{11} particles of AdCMV–β-Gal (lanes 4, 5, 9, and 10) or 2 × 10^{11} particles of AdCMV-RAP (lanes 2, 3, 7 and 8) was obtained 5 days after virus administration. Samples (0.5 μl) were separated by SDS–gel electrophoresis on 4 to 15% polyacrylamide gels under reducing conditions, and the proteins were transferred to nitrocellulose filters. Filters were incubated with polyclonal rabbit IgGs (5 μg/ml) directed against apoB (B-100 and B-48), apoE (E), apoAI (AI), or RAP. Bound IgG was detected with ^{125}I-labeled goat antibody to rabbit IgG (1 × 10^6 cpm/ml) as described (*13*). The blots were then exposed to Kodak XAR film. Exposure times for lanes 1 to 5 were 2 hours for B-100 and B-48, 4 hours for AI, and 16 hours for E and RAP; for lanes 6 to 10, exposure times were 1 hour for B-100 and B-48, E, and RAP and 2 hours for AI.

chronic defect in remnant clearance) also have substantially lower HDL cholesterol concentrations than normal animals, suggesting a functional connection between HDL and remnant metabolism.

In conclusion, the results presented in this study provide additional evidence for a physiological dual role of LRP in the metabolism of lipoproteins and proteases. Furthermore, our results have demonstrated the usefulness of adenovirus-mediated gene transfer to overexpress a dominant negative regulator and to study the physiological consequences of the transient inactivation of the target protein in an intact animal. Such an approach may be generally applicable for the in vivo inactivation and study of other developmentally essential genes (such as growth factors, signaling receptors, or transcription factors) for which dominant negative mutants or antagonists exist.

REFERENCES AND NOTES

1. E. J. Schaefer *et al.*, *J. Clin. Invest.* **78**, 1206 (1986).
2. A. S. Plump *et al.*, *Cell* **71**, 343 (1992); S. H. Zhang, R. L. Reddick, J. A. Piedrahita, N. Maeda, *Science* **258**, 468 (1992).
3. E. E. T. Windler, J. Greeve, W. H. Daerr, H. Greten, *Biochem. J.* **252**, 553 (1988); S. Y. Choi and A. D. Cooper, *J. Biol. Chem.* **268**, 15804 (1993); Y. Nagata, J. Chen, A. D. Cooper, *ibid.* **263**, 15151 (1988).
4. R. W. Mahley and M. M. Hussain, *Curr. Opin. Lipidol.* **2**, 170 (1991).
5. D. C. Rubinsztein *et al.*, *J. Clin. Invest.* **86**, 1306 (1990); T. Kita *et al.*, *Proc. Natl. Acad. Sci. U.S.A.* **79**, 3623 (1982).
6. S. Ishibashi *et al.*, *J. Clin. Invest.* **92**, 883 (1993).
7. J. Herz *et al.*, *EMBO J.* **7**, 4119 (1988); M. M. Hussain *et al.*, *J. Biol. Chem.* **266**, 13936 (1991); R. C. Kowal, J. Herz, J. L. Goldstein, V. Esser, M. S. Brown, *Proc. Natl. Acad. Sci. U.S.A.* **86**, 5810 (1989); R. C. Kowal *et al.*, *J. Biol. Chem.* **265**, 10771 (1990); U. Beisiegel, W. Weber, G. Bengtsson-Olivecrona, *Proc. Natl. Acad. Sci. U.S.A.* **88**, 8342 (1991); U. Beisiegel, W. Weber, G. Ihrke, J. Herz, K. K. Stanley, *Nature* **341**, 162 (1989).
8. M. S. Brown, J. Herz, R. C. Kowal, J. L. Goldstein, *Curr. Opin. Lipidol.* **2**, 65 (1991).
9. J. Herz, D. E. Clouthier, R. E. Hammer, *Cell* **71**, 411 (1992); *ibid.* **73**, 428 (1993).
10. D. K. Strickland *et al.*, *J. Biol. Chem.* **265**, 17401 (1990); T. Kristensen *et al.*, *FEBS Lett.* **276**, 151 (1990).
11. A. Nykjaer *et al.*, *J. Biol. Chem.* **267**, 14543 (1992); G. Bu, S. Williams, D. K. Strickland, A. L. Schwartz, *Proc. Natl. Acad. Sci. U.S.A.* **89**, 7427 (1992); K. Orth, E. L. Madison, M.-J. Gething, J. F. Sambrook, J. Herz, *ibid.*, p. 7422; M. Z. Kounnas, J. Henkin, W. S. Argraves, D. K. Strickland, *J. Biol. Chem.* **268**, 21862 (1993).
12. S. K. Moestrup and J. Gliemann, *J. Biol. Chem.* **266**, 14011 (1991).
13. J. Herz, J. L. Goldstein, D. K. Strickland, Y. K. Ho, M. S. Brown, *ibid.*, p. 21232.
14. S. E. Williams, J. D. Ashcom, W. S. Argraves, D. K. Strickland, *ibid.* **267**, 9035 (1992).
15. I. Warshawsky, G. Bu, A. L. Schwartz, *J. Clin. Invest.* **92**, 937 (1993).
16. L. D. Stratford-Perricaudet, I. Makeh, M. Perricaudet, P. Briand, *ibid.* **90**, 626 (1992); T. A. G. Smith *et al.*, *Nat. Genet.* **5**, 397 (1993).
17. J. Herz and R. D. Gerard, *Proc. Natl. Acad. Sci. U.S.A.* **90**, 2812 (1993).
18. Recombinant adenovirus expressing the full-length rat RAP cDNA (AdCMV-RAP) was constructed by a modification of the procedure described in (*17*). Briefly, a plasmid containing the left inverted repeat and sequences from map unit 0 to 1.3 of adenovirus 5 (Ad5), a cytomegalovirus (CMV) promoter, the RAP cDNA, and the 3′-untranslated region of bovine growth hormone (bpA) was linearized at a unique Xba I site downstream of bpA and ligated to adenovirus sequences extending from map units 9.1 to 100 of the Ad5 derivative, AdRR5. 293 cells were transfected with the ligation mixture, and recombinant viruses containing RAP were identified by polymerase chain reaction. AdCMV–β-Gal, AdCMV-Luc, and procedures of virus preparation were as described (*17*). Three independent AdCMV-RAP isolates were used and gave equivalent results. Virus preparations were titrated on 293 cells. Plaque-forming units (PFU) were related to viral particle numbers and were similar for independent virus preparations (2×10^{11} particles $\approx 5 \times 10^9$ PFU).
19. Human methylamine-activated α_2M and bovine asialofetuin (Sigma) were iodinated by the Iodogen procedure (*13*). Wild-type or LDLR$^{-/-}$ C57BL/6J × 129SvJ hybrid male mice were bred in house and fed ad libitum throughout the course of the experiment (Teklad 4% Mouse/Rat Diet 7001, Harlan Teklad Premier Laboratory Diets). Before virus injection and turnover studies, animals were anesthetized by intraperitoneal sodium pentobarbital (Nembutal) injection (~80 μg per gram of body weight). Viruses or iodinated protein were slowly injected into the external jugular vein in a total volume of 200 to 250 μl of tris-buffered saline. Animal care and experimental procedures involving animals were conducted in accordance with institutional guidelines.
20. G. Ashwell and J. Harford, *Annu. Rev. Biochem.* **51**, 531 (1982).
21. R. J. Havel and J. P. Kane, in *The Metabolic Basis of Inherited Disease*, C. R. Scriver, A. L. Beaudet, W. S. Sly, D. Valle, Eds. (McGraw-Hill, New York, 1989), pp. 1129–1138; J. Scott, *Mol. Biol. Med.* **6**, 65 (1989); L. Chan, *J. Biol. Chem.* **267**, 25621 (1992).
22. H. S. Ginsberg *et al.*, *Proc. Natl. Acad. Sci. U.S.A.* **88**, 1651 (1991); S. P. Goff and T. Shenk, *Curr. Opin. Genet. Dev.* **3**, 71 (1993).
23. T. E. Willnow and J. Herz, unpublished observations.
24. Z.-S. Ji *et al.*, *J. Biol. Chem.* **268**, 10160 (1993).
25. S. Shafi, S. E. Brady, A. Bensadoun, R. J. Havel, *J. Lipid. Res.* **35**, 709 (1994).
26. R. L. Hamilton, J. S. Wong, L. S. S. Guo, S. Krisans, R. J. Havel, *J. Lipid Res.* **31**, 1589 (1990).
27. H. Mokuno, S. Brady, L. Kotite, J. Herz, R. J. Havel, *J. Biol. Chem.* **269**, 13238 (1994).
28. R. A. Orlando, D. Kerjaschki, H. Kurihura, D. Biemesderfer, M. G. Farquhar, *Proc. Natl. Acad. Sci. U.S.A.* **89**, 6698 (1992).
29. J. Herz, *Curr. Opin. Lipidol.* **4**, 107 (1993).
30. R. C. LeBoeuf *et al.*, *J. Lipid Res.* **31**, 91 (1990).
31. W. Gamble, M. Vaughan, H. S. Kruth, J. Avigan, *ibid.* **19**, 1068 (1978).

32. We thank R. Havel, D. Russell, M. Brown, and J. Goldstein for critical reading of the manuscript and for helpful comments; W.-L. Niu and S. Clark for technical assistance; and D. Strickland for providing human methylamine-activated α_2M. Supported by grants from the NIH (HL20948), the Keck Foundation, and the Perot Family Foundation. T.E.W. and S.I. are recipients of a postdoctoral fellowship from the Deutsche Forschungsgemeinschaft and from the Sasakawa Health Science Foundation, Tokyo, respectively. J.H. is supported by the Syntex Scholar Program and is a Lucille P. Markey Scholar.

13 January 1994; accepted 13 April 1994

De Novo and Inherited Deletions of the 5q13 Region in Spinal Muscular Atrophies

Judith Melki, Suzie Lefebvre, Lydie Burglen, Philippe Burlet, Olivier Clermont, Philippe Millasseau, Sophie Reboullet, Bernard Bénichou, Massimo Zeviani, Denis Le Paslier, Daniel Cohen, Jean Weissenbach, Arnold Munnich*

Spinal muscular atrophies (SMAs) represent the second most common fatal autosomal recessive disorder after cystic fibrosis. Childhood spinal muscular atrophies are divided into severe (type I) and mild forms (types II and III). By a combination of genetic and physical mapping, a yeast artificial chromosome contig of the 5q13 region spanning the disease locus was constructed that showed the presence of low copy repeats in this region. Allele segregation was analyzed at the closest genetic loci detected by markers C212 and C272 in 201 SMA families. Inherited and de novo deletions were observed in nine unrelated SMA patients. Moreover, deletions were strongly suggested in at least 18 percent of SMA type I patients by the observation of marked heterozygosity deficiency for the loci studied. These results indicate that deletion events are statistically associated with the severe form of spinal muscular atrophy.

Proximal spinal muscular atrophies (incidence: 1 out of 6000 newborns) (*1–4*) are characterized by degeneration of anterior horn cells of the spinal cord, leading to progressive symmetrical limb and trunk paralysis associated with muscular atrophy. The childhood spinal muscular atrophies are divided into types I (Werdnig-Hoffmann disease), II, and III (Kugelberg-Welander disease) on the basis of age of onset, milestones of development, and life span (*5*). By means of linkage analysis, we and others have shown that all three forms of spinal muscular atrophy map to chromosome 5q11.2–q13.3 (*6–9*).

J. Melki, S. Lefebvre, L. Burglen, P. Burlet, O. Clermont, S. Reboullet, B. Bénichou, M. Zeviani, A. Munnich, Unité de Recherches sur les Handicaps Génétiques de l'Enfant, INSERM U-393, Hôpital des Enfants-Malades, 75743 Paris, France.
P. Millasseau and J. Weissenbach, Genethon, Evry, France.
D. Le Paslier and D. Cohen, Centre d'Etudes du Polymorphisme Humain (CEPH), Paris, France.

*To whom correspondence should be addressed.